TITLE: Test Cases for a Rectangular Supercritical Wing Undergoing Pitching Oscillations

6E. TEST CASES FOR A RECTANGULAR SUPERCRITICAL WING UNDERGOING PITCHING OSCILLATIONS

Submitted by

Robert M. Bennett
Senior Aerospace Engineer
Aeroelasticity Branch, Structures and Materials
Mail Stop 340
NASA Langley Research Center
Hampton, VA 23681-2199 USA
r.m.bennett@larc.nasa.gov

INTRODUCTION

Steady and unsteady measured pressures for a Rectangular Supercritical Wing (RSW) undergoing pitching oscillations have been presented in Ref 1 to 3. From the several hundred compiled data points, 27 static and 36 pitching oscillation cases have been proposed for computational Test Cases to illustrate the trends with Mach number, reduced frequency, and angle of attack.

The wing was designed to be a simple configuration for Computational Fluid Dynamics (CFD) comparisons. The wing had an unswept rectangular planform plus a tip of revolution, a panel aspect ratio of 2.0, a twelve per cent thick supercritical airfoil section, and no twist. The model was tested over a wide range of Mach numbers, from 0.27 to 0.90, corresponding to low subsonic flows up to strong transonic flows. The higher Mach numbers are well beyond the design Mach number such as might be required for flutter verification beyond cruise conditions. The pitching oscillations covered a broad range of reduced frequencies.

Some early calculations for this wing are given for lifting pressure in Ref 3 and 4 as calculated from a linear lifting surface program and from a transonic small perturbation program. The unsteady results were given primarily for a mild transonic condition at $M = 0.70$. For these cases the agreement with the data was only fair, possibly resulting from the omission of viscous effects. Supercritical airfoil sections are known to be sensitive to viscous effects (for example, one case cited in Ref 4). Calculations using a higher level code with the full potential equations have been presented in Ref 5 for one of the same cases, and with the Euler equations in Ref 6. The agreement around the leading edge was improved, but overall the agreement was not completely satisfactory. Typically for low-aspect-ratio rectangular wings, transonic shock waves on the wing tend to sweep forward from root to tip such that there are strong three-dimensional effects. It might also be noted that for most of the test, the model was tested with free transition, but a few points were taken with an added transition strip for comparison. Some unpublished results of a rigid wing of the same airfoil and planform that was tested on the pitch and plunge apparatus mount system (PAPA, Ref 7-8) showed effects of the lower surface transition strip on flutter at the lower subsonic Mach numbers. Significant effects of a transition strip were also obtained on a wing with a thicker supercritical section on the PAPA mount system (Ref 9). Both of these flutter tests on the PAPA resulted in very low reduced frequencies that may be a factor in this influence of the transition strip. However, these results indicate that correlation studies for RSW may require some attention to the estimation of transition location to accurately treat viscous effects.

In this report several Test Cases are selected to illustrate trends for a variety of different conditions with emphasis on transonic flow effects. An overview of the model and tests is given and the standard formulary for these data is listed. Sample data points are presented in both tabular and graphical form. A complete tabulation and plotting of all the Test Cases is given in Ref 10. Only the static pressures and the real and imaginary parts of the first harmonic of the unsteady pressures are available. All the data for the test are available in electronic file form and are printed in the tables of Ref 1. The Test Cases are also available as separate electronic files.

LIST OF SYMBOLS AND DEFINITIONS

c	local chord
c_r	wing root chord, ft (m)
C_p	pressure coefficient, $(p - p_\infty)/q_\infty$ steady; $(p - p_{mean})/q_\infty$ unsteady
f	frequency, Hz
H_o	freestream total pressure, psf (kPa)
k	reduced frequency, $\omega c_r/(2V_\infty)$
M	Mach number
p	pressure, psf (kPa)
p_{mean}	mean local pressure, psf (kPa)
p_∞	freestream static pressure, psf (kPa)
q_∞	dynamic pressure, psf (kPa)

R	local radius of tip section
Rn	Reynolds number based on chord
s	semispan
T_o	total or stagnation temperature, °R (°C)
V_∞	freestream velocity, ft/sec (m/sec)
x	streamwise distance from leading edge
x/c	steamwise fraction of local chord
y	spanwise coordinate normal to freestream
z_u, z_l	airfoil vertical upper and lower ordinate normal to freestream, positive up
α_o	mean angle of attack, degrees
θ	amplitude of pitch oscillations, degrees or radians
η	fraction of span, y/s
γ	ratio of specific heats for test gas
ω	frequency, radians/second

MODEL AND TESTS

The rectangular supercritical wing model was tested in the NASA Langley Transonic Dynamics Tunnel (TDT). The tunnel has a slotted test section 16-feet (4.064 m) square with cropped corners. At the time of these tests, it could be operated with air or a heavy gas, R-12, as a test medium at pressures from very low to near atmospheric values. Currently the TDT can be operated with air or R-134a as a test medium. An early description of this facility is given in Ref 11 and the early data system in Ref 12. More recent descriptions of the facility are given in Ref 13-14, and of the recent data system in Ref 15 and 16. Based on cone transition results (Ref 17-18), the turbulence level for this tunnel is in the "average large transonic tunnel" category. Some low speed turbulence measurements in air have also been presented in Ref 19.

A photograph of the model and splitter plate as installed in the TDT is shown in Fig 1 and the dimensions of the model and splitter plate setup are detailed in the sketch of Fig 2. The unswept rectangular planform was 48 inches (1219 mm) in span plus a tip of revolution of maximum radius of 1.434 inches (36.4 mm) such that the maximum spanwise extent was 49.43 inches (1255 mm). The chord was 24 inches (609.6 mm). The model was mounted on a splitter plate offset from the wall. It was oscillated in pitch about 46 percent root chord with a shaft that was directly driven by a rotary hydraulic actuator located behind the tunnel wall. It could be set at various mean angles, and the amplitude and frequency of oscillation could be varied.

The wing was constructed in three sections. The center section was made of aluminum with the upper and lower halves pinned and bonded together. The leading and trailing edge portions were made of balsa and Kevlar sandwich material to minimize the inertia loading. The leading and trailing edge sections were joined at 0.23 and 0.69 of the chord, respectively. Some stiffness measurements are given in Ref 3.

Unsteady pressures were measured on four chords. There were 14 measurement locations along each chord on both upper and lower surfaces and one location in the nose for a total of 29 points per chord as shown in Fig 3 and listed in Table 1. The transducers in the center portion of the wing were in-situ measurements. The transducers in the leading and trailing edges were mounted near the joints of the leading or trailing edge sections to the center beam. Equal length tubes were used between the orifices and these transducers. Other transducers were located by the first row of in-situ transducers and had tubes of the same length located in the center beam. These transducers were used to correct for dynamic effects of the tubes of the transducers in the leading and trailing edges. Each transducer was referenced to the tunnel static pressure and was used to measure both static and unsteady pressures. Eight accelerometers were located on the center section for dynamic measurements. Fig 4 (from Ref 1) shows C_L versus Mach number as integrated from the pressure data, and gives an overall indication of the performance of the wing.

The airfoil for the RSW is illustrated in Fig 5. This airfoil was derived by ratioing the thickness of an 11 percent airfoil (Ref 20) to 12 percent while keeping the same mean camber line. The trailing edge thickness was increased to 0.7 percent chord by rotating the lower cusp area as described in Ref 21. The design Mach number and lift coefficient for the 2-dimensional airfoil is quoted as M = 0.80, and C_L = 0.6 (Ref 3). The design ordinates and the measured ordinates for five spanwise stations are given in Table 2. The design wing tip-shape is also presented in Table 2. The quoted accuracy of the measured ordinates is .00040 in. (.0010 mm). The measured airfoil ordinates are compared with the theoretical ordinates in Fig 6. The measured ordinates agree very well with the theoretical ones but with some small deviation in the lower surface aft, or cove, region.

By CFD standards, the theoretical and measured ordinates were given on a medium to coarse grid. In order to develop a common set of ordinates for CFD applications, the measured ordinates have been interpolated at each span station. The measured ordinates were fit with a spline using arc-length as the independent parameter and running from upper surface trailing edge around the nose to the lower surface trailing edge. Three passes of a local 5-point least-squares cubic smoothing patch were made, and the resulting curve interpolated for the ordinates. These smoothed ordinates at the five span stations were interpolated for 206 values of x/c for each span station and included as a file for the data set. They are also listed in a table in Ref 10. One airfoil section after smoothing and the corresponding streamwise slopes are presented in Fig 7. For this wing, the

measured spanwise sections are nearly identical, except at the lower surface trailing edge where the slope varies by about 8 per cent. It should also be noted that the slope varies quite rapidly near the inflection point in the cove region of the airfoil lower surface (Fig 7).

As can been seen in Fig 1, the model was tested with the sidewall slots of the test section open. Some recent unpublished results for a model having about six times the root chord of this model and mounted directly to the wind tunnel wall, have shown an influence of closing the slots on static lift curve slope of the order of ten percent (similar to those measured in Ref 22). Significantly less influence would be anticipated for this much smaller model mounted on a splitter plate.

TEST CASES

The static Test Cases for the rectangular supercritical wing are given in Table 3, and the dynamic Test Cases are presented in Table 4. The point number is used to identify the test conditions and are in the order taken during the test. The cases are chosen to indicate trends with Mach number at two degrees angle of attack, and also at zero and four degrees angle of attack with a coarse increment. Some cases for high angles of attack at M=0.40, some cases for the effect of transition at M=0.825, and some cases for air as the test medium are listed. The dynamic cases are chosen to evaluate unsteady effects at these static conditions. The cases illustrate variations with Mach number for nearly constant reduced frequency, and variations with reduced frequency at constant Mach numbers. Some cases are chosen also to indicate the effects of angle of attack, transition strip, and amplitude. The plot of C_L versus Mach number as integrated from the pressure data (Fig 4) was used as a guide in selecting the Test Cases.

Sample data for the static Test Cases are tabulated and shown in composite plots in Fig 8. Sample data for the dynamic cases are also tabulated and shown in the plots of Fig 9 in terms of in-phase and out-of-phase parts (real and imaginary) of the pressure normalized by the amplitude of the pitching oscillation. The phase is referenced to the pitching motion. More digits than are significant are retained in the tables to accurately reproduce the phase angles of the original tabulations. No further screening of bad transducer output points have been performed in this report.

The files included on the CD-ROM are ascii files and a readme file is included. The file for the static data is named rswstat and a Fortran subprogram to read it, rswstrd.f, is furnished. The dynamic data is on file rswdynmc and the subprogram to read it is rswdyrd.f. The data files consist of contiguous data points in the format shown in the figures. Both theoretical and measured ordinates are given in file rsword and the interpolated and smoothed ordinates are given in file rswordint.

Note that most of the tests for RSW were conducted with the heavy gas, R-12, as the test medium. The ratio of specific heats, γ, is tabulated for each point in the figures. It varies from about 1.129 to 1.132 and a value of 1.132 is suggested for use in computational comparisons. The corresponding value of Prandtl number is calculated to range from 0.77 to 0.78 for the conditions of this test assuming 0.99 for the fraction of heavy gas in the heavy gas-air mixture.

FORMULARY

1 General Description of Model

1.1	Designation	Rectangular Supercritical Wing (RSW)
1.2	Type	Semispan wing
1.3	Derivation	None
1.4	Additional remarks	Shown mounted in tunnel in Fig 1 and setup sketched in Fig 2
1.5	References	Ref 1-3 are the original sources

2 Model Geometry

2.1	Planform	Rectangular plus tip of revolution
2.2	Aspect ratio	2.0 for panel (without tip)
2.3	Leading edge sweep	Unswept
2.4	Trailing edge sweep	Unswept
2.5	Taper ratio	1.0
2.6	Twist	None
2.7	Wing centreline chord	24.0 inches (609.6 mm)
2.8	Semi-span of model	48.0 inches (1219 mm)plus tip
2.9	Area of planform	1152 sq. in (1.786 sq m)
2.10	Location of reference sections and definition of profiles	See Table 2, Fig 5-7, and files rsword and rswordint
2.11	Lofting procedure between reference sections	Constant percent thickness airfoil
2.12	Form of wing-body junction	No fairing

2.13	Form of wing tip	Tip of rotation. Each spanwise section formed by half circle with radius half the local thickness and rotated about the mean line
2.14	Control surface details	No control surfaces
2.15	Additional remarks	See Fig 1-3 for overview
2.16	References	Ref 1-3

3 Wind Tunnel

3.1	Designation	NASA LaRC Transonic Dynamics Tunnel (TDT)
3.2	Type of tunnel	Continuous flow, single return
3.3	Test section dimensions	16 ft x 16 ft (4.064 x 4.064 m)
3.4	Type of roof and floor	Three slots each
3.5	Type of side walls	Two sidewall slots
3.6	Ventilation geometry	Constant width slots in test region
3.7	Thickness of side wall boundary layer	Some documentation in Ref 11. Model tested with splitter plate
3.8	Thickness of boundary layers at roof and floor	Not documented
3.9	Method of measuring velocity	Calculated from static pressures measured in plenum and total pressure measured upstream of entrance nozzle of test section
3.10	Flow angularity	Not documented, considered small
3.11	Uniformity of velocity over test section	Not documented, considered nearly uniform
3.12	Sources and levels of noise or turbulence in empty tunnel	Generally unknown. Some low speed measurements are presented in Ref 19. Cone transition measurements are presented in Ref 17 and 18
3.13	Tunnel resonances	Unknown
3.14	Additional remarks	Tests generally performed in heavy gas, R-12. Ratio of specific heats, γ, is 1.129-1.132. For computations, 1.132 is recommended. For the conditions of this test, the Prandtl number is calculated to be 0.77-0.78
3.15	References on tunnel	Ref 11, 13, and 14

4 Model Motion

4.1	General description	Pitching about 46% of root chord for wing, 11.04 inches (280.4 mm) aft of leading edge
4.2	Reference coordinate and definition of motion	Pitch about axis normal to freestream
4.3	Range of amplitude	Pitch amplitude of 0.50, 1.00, and 1.50 degrees
4.4	Range of frequency	5, 10, 15, and 20 Hz with a few lower frequencies
4.5	Method of applying motion	Pitch oscillations shaft-driven with a rotary hydraulic actuator
4.6	Timewise purity of motion	Not documented
4.7	Natural frequencies and normal modes of model and support system	First natural frequency was 34.8 Hz; maximum test frequency was 20 Hz
4.8	Actual mode of applied motion including any elastic deformation	Some accelerometer measurements given in Ref 2. Elastic deformations not expected to be significant, but stiffness measurements available in Ref 3
4.9	Additional remarks	None

5 Test Conditions

5.1	Model planform area/tunnel area	.03
5.2	Model span/tunnel height	.25
5.3	Blockage	Model less than 0.4%
5.4	Position of model in tunnel	Mounted from splitter plate on wall and in the center of the tunnel

5.5 Range of Mach number	0.40 to 0.90
5.6 Range of tunnel total pressure	175 to 2025 psf (8.38 to 812 kPa)
5.7 Range of tunnel total temperature	Not documented but generally in the range of 520 to 580 degrees Rankine (16 to 49° C)
5.8 Range of model steady or mean incidence	Generally -1 to 7 degrees, a few points from -4 to 14 degrees
5.9 Definition of model incidence	From chord line or wing reference plane of airfoil, see Fig 5-7
5.10 Position of transition, if free	Unknown except for a few points with transition strip. Although the joint was quite smooth, an initial estimate of transition might be considered to be at the joint between the leading edge section and the main spar (23 per cent chord)
5.11 Position and type of trip, if transition fixed	Generally free transition. A few points measured with transition strip of number 60 grit located at 6 percent chord on upper and lower surfaces (number is approximate grains per inch (per 25.4 mm)).
5.12 Flow instabilities during tests	None defined
5.13 Changes to mean shape of model due to steady aerodynamic load	Not measured
5.14 Additional remarks	Generally, a heavy gas, R-12, was used as a test medium for the Test Cases. The ratio of specific heats, γ, is tabulated for each point and varies from about 1.129 to 1.132. A value of 1.132 is suggested for use in computational comparisons. The corresponding value of Prandtl number is 0.77-0.78. A few points were also measured in air
5.15 References describing tests	Ref 1- 3

6 Measurements and Observations

6.1 Steady pressures for the mean conditions	yes
6.2 Steady pressures for small changes from the mean conditions	yes
6.3 Quasi-steady pressures	no
6.4 Unsteady pressures	yes
6.5 Steady section forces for the mean conditions by integration of pressures	no
6.6 Steady section forces for small changes from the mean conditions by integration	no
6.7 Quasi-steady section forces by integration	no
6.8 Unsteady section forces by integration	no
6.9 Measurement of actual motion at points of model	no
6.10 Observation or measurement of boundary layer properties	no
6.11 Visualisation of surface flow	no
6.12 Visualisation of shock wave movements	no
6.13 Aditional remarks	no

7 Instrumentation

7.1 Steady pressure

7.1.1 Position of orifices spanwise and chordwise	29 chordwise locations at 4 spanwise stations. See Fig 3
7.1.2 Type of measuring system	Kulite

7.2 Unsteady pressure

7.2.1 Position of orifices spanwise and chordwise	Same transducers measured steady and unsteady pressures

7.2.2 Diameter of orifices	Not documented
7.2.3 Type of measuring system	In situ pressure gages and short tubes to unsteady gages with tube calibrations
7.2.4 Type of transducers	Kulites
7.2.5 Principle and accuracy of calibration	Statically calibrated through reference tubes
7.3 Model motion	
7.3.1 Method of measuring motion reference coordinate	Potentiometer
7.3.2 Method of determining spatial mode of motion	Some verification with accelerometers
7.3.3 Accuracy of measured motion	Undocumented
7.4 Processing of unsteady measurements	
7.4.1 Method of acquiring and processing measurements	Analog signals digitized at about 300 samples/sec for 75-100 cycles depending on frequency
7.4.2 Type of analysis	Fourier analysis
7.4.3 Unsteady pressure quantities obtained and accuracies achieved	Amplitude and phase of each pressure signal. Accuracy not specified
7.4.4 Method of integration to obtain forces	None
7.5 Additional remarks	None
7.6 References on techniques	Data system overview for test given in Ref 12

8 Data Presentation

8.1 Test Cases for which data could be made available	See Ref 2
8.2 Test Cases for which data are included in this document	See Tables 3 and 4
8.3 Steady pressures	Generally available for each Test Case
8.4 Quasi-steady or steady perturbation pressures	Steady pressures measured for several angles of attack
8.5 Unsteady pressures	Primary data. First harmonic only. No time histories or mean values saved. C_p magnitude and phase of Ref 2 converted to real and imaginary parts and normalised by amplitude of oscillation (in radians) for this report.
8.6 Steady forces or moments	None
8.7 Quasi-steady or unsteady perturbation forces	None
8.8 Unsteady forces and moments	None
8.9 Other forms in which data could be made available	None
8.10 References giving other representations of data	Ref 1-6

9 Comments on Data

9.1 Accuracy	
9.1.1 Mach number	Not documented
9.1.2 Steady incidence	Not documented
9.1.3 Reduced frequency	Should be accurate
9.1.4 Steady pressure coefficients	Not documented
9.1.5 Steady pressure derivatives	None
9.1.6 Unsteady pressure coefficients	Not documented, but each gage individually calibrated dynamically and monitored statically

9.2	Sensitivity to small changes of parameter	None indicated. Amplitudes of oscillation was varied in test
9.3	Non-linearities	Many flow conditions involve shock waves
9.4	Influence of tunnel total pressure	Some variation during test. Most of the test at constant dynamic pressure
9.5	Effects on data of uncertainty, or variation, in mode of model motion	Unknown, not expected to be appreciable.
9.6	Wall interference corrections	None applied
9.7	Other relevant tests on same model	None
9.8	Relevant tests on other models of nominally the same shapes	None
9.9	Any remarks relevant to comparison between experiment and theory	Generally free transition. R_n from $1x10^6$ to 8×10^6 but generally about 4×10^6. Test Reynolds number included for each Test Case
9.10	Additional remarks	Upper and lower surfaces instrumented symmetrically. Reduced frequency based on root semichord, 12.0 inches (304.8 mm)
9.11	References on discussion of data	Ref 1-6

10 Personal Contact for Further Information

Head, Aeroelasticity Branch
Mail Stop 340
NASA Langley Research Center
Hampton, VA 23681-2199 USA

Phone: +1-(757)-864-2820
FAX: +1-(757)-864-8678

LIST OF REFERENCES

1. Ricketts, Rodney H.; Sandford, Maynard C.; Seidel, David A.; and Watson, Judith J: *Transonic Pressure Distributions on a Rectangular Supercritical Wing Oscillated in Pitch.* Journal of Aircraft, vol. 21, no. 8, August 1984, pp 576-582. (Also AIAA Paper 83-0923, May 1983 which is available as NASA TM 84616, Mar. 1983).

2. Ricketts, Rodney H.; Sandford, Maynard C.; Watson, Judith J.; and Seidel, David A.: *Subsonic and Transonic Unsteady- and Steady-Pressure Measurements on a Rectangular Supercritical Wing Oscillated in Pitch.* NASA TM 85765, August 1984.

3. Ricketts, Rodney H.; Sandford, Maynard C.; Watson, Judith J.; and Seidel, David A.: *Geometric and Structural Properties of a Rectangular Supercritical Wing Oscillated in Pitch for Measurements of Unsteady Transonic Pressure Distributions.* NASA TM 85673, Nov. 1983.

4. Seidel, David A.; Bennett, Robert M.; and Ricketts, Rodney H.: *Some Recent Applications of XTRAN3S.* AIAA Paper 83-1811, July 1983. (Also available as NASA TM 85641, May 1983).

5. Hounjet, M. H. L.: *NLR Inviscid Transonic Unsteady Loads Prediction Methods in Aeroelasticity.* Paper No. 12 in "Transonic Unsteady Aerodynamics and Aeroelasticity," AGARD CP-507, March 1992.

6. Brenneis, A.; and Eberle, A.: *Application of an Implicit Relaxation Method Solving the Euler Equations for Time-Accurate Unsteady Problems.* Journal of Fluids Engineering, Transactions of the ASME, Vol 112, Dec. 1990, pp. 510-520.

7. Farmer, Moses G.: *A Two-Degree-of Freedom Flutter Mount System with Low Damping for Testing Rigid Wings at Different Angles of ttack.* NASA TM 83302, 1982.

8. Farmer, Moses G.: *Model Mount System for Testing Flutter.* U. S. Patent No. 4,475,385, Oct. 9, 1984.

9. Dansberry, B.E.; Durham, M.H.; Bennett, R.M.; Rivera, J.A., Jr.; Silva, W.A.; Wieseman, C.D.; and Turnock, D.L.: *Experimental Unsteady Pressures at Flutter on the Supercritical Wing Benchmark Model.* AIAA Paper No. 93-1592, April 1993.

10. Bennett, Robert M.; Walker, Charlotte, E.: *Computational Test Cases for a Rectangular Supercritical Wing Undergoing Pitching Oscillations.* NASA/TM-1999-209130, Apr. 1999.

11. Aeroelasticity Branch Staff: *The Langley Transonic Dynamics Tunnel.* LWP-799, Sep. 1969.

12. Cole, Patricia H.: *Wind Tunnel Real-Time Data Acquisition System.* NASA TM-80081, 1979.

13. Cole, Stanley C., and Rivera, Jose, A., Jr.: *The New Heavy Gas Testing Capability in the NASA Langley Transonic Dynamics Tunnel.* Paper No. 4, presented at the Royal Aeronautical Society Wind Tunnels and Wind Tunnel Test Techniques Forum, Churchill College, Cambridge, UK, Apr. 1997.

14. Corliss, James M.; and Cole, Stanley R.: *Heavy Gas Conversion of the NASA Langley Transonic Dynamics Tunnel.* AIAA Paper 98-2710, June 1998.

15. Wieseman, Carol D.; and Hoadley, Sherwood, T.: *Versatile Software Package for Near Real-Time Analysis of Experimental Data.* AIAA Paper 98-2722, June 1998.

16. Bryant, C.; and Hoadley, S. T.: Open Architecture Dynamic Data System at Langley's Transonic Dynamics Tunnel. AAIA Paper 98-0343, Jan. 1998.

17. Dougherty, N. Sam, Jr.: *Influence of Wind Tunnel Noise on the Location of Boundary-Layer Transition on a Slender Cone at Mach Numbers from 0.2 to 5.5.* Volume I. - Experimental Methods and Summary of Results. Volume II. - Tabulated and Plotted Data. AEDC --TR-78-44, March 1980.

18. Dougherty, N. S., Jr.; and Fisher, D. F.: *Boundary-Layer Transition on a 10-Degree Cone: Wind Tunnel/Flight Correlation.* AIAA Paper 80-0154, January 1980.

19. Sleeper, Robert K.; Keller, Donald F.; Perry, Boyd, III; and Sandford, Maynard C.: *Characteristics of Vertical and Lateral Tunnel Turbulence Measured in Air in the Langley Transonic Dynamics Tunnel.* NASA TM 107734, March 1993.

20. Whitcomb, Richard T.: *Review of NASA Supercritical Airfoils.* ICAS Paper No.74-10, presented at the Ninth Congress of the International Council of The Aeronautical Sciences, Aug. 1974, Haifa, Israel.

21. Harris, Charles D.: *Wind-Tunnel Investigation of Effects of Trailing-Edge Geometry on a NASA Supercritical Airfoil Section.* NASA TM X-2336, Sept. 1971.

22. Lambourne, N.; Destuynder, R.; Kienappel, K.; and Roos, R.: *Comparative Measurements in Four European Wind Tunnels of the Unsteady Pressures on an Oscillating Model (The NORA Experiments).* AGARD Report No. 673, Feb. 1980.

ACKNOWLEDGMENT

Appreciation is extended to David A. Seidel of the Boeing Company, Seattle WA, USA for making the data files available from the NASA Langley archives. The considerable assistance of Charlotte E. Walker in generating the tables and figures for this report is also gratefully acknowledged.

Table 1. Pressure Orifice Locations and Type

x/c	Type
0.000	Tube to Transducer
.003	Tube to Transducer
.050	Tube to Transducer
.100	Tube to Transducer
.200	Tube to Transducer
.260	In Situ
.320	In Situ
.380	In Situ
.440	In Situ
.500	In Situ
.560	In Situ
.620	In Situ
.700	Tube to Transducer
.800	Tube to Transducer
.900	Tube to Transducer

Table 2. Design and Measured Ordinates

		Design Values		Measured Values					
				y = 1.000 in		y = 14.932 in		y = 28.324 in	
x, in	x/c	z_u, in	z_l, in	z_u, in	z_l, in	z_u, in	z_l, in	z_u, in	z_l, in
0.0000	0.0000	0.0000	0.0000	0.0000	0.0000	0.0000	0.0000	0.0000	0.0000
0.1800	0.0075	0.4610	-0.4610	0.4571	-0.4726	0.4535	-0.4701	0.4514	-0.4624
0.3000	0.0125	0.5630	-0.5650	0.5602	-0.5750	0.5557	-0.5717	0.5572	-0.5669
0.6000	0.0250	0.7230	-0.7350	0.7193	-0.7435	0.7156	-0.7376	0.7197	-0.7380
0.9000	0.0375	0.8280	-0.8470	0.8226	-0.8569	0.8234	-0.8498	0.8242	-0.8492
1.2000	0.0500	0.9100	-0.9360	0.9050	-0.9436	0.9050	-0.9383	0.9062	-0.9365
1.8000	0.0750	1.0330	-1.0670	1.0289	-1.0720	1.0290	-1.0693	1.0295	-1.0683
2.4000	0.1000	1.1220	-1.1610	1.1191	-1.1638	1.1176	-1.1620	1.1176	-1.1603
3.0000	0.1250	1.1930	-1.2340	1.1901	-1.2372	1.1895	-1.2345	1.1910	-1.2346
3.6000	0.1500	1.2480	-1.2890	1.2466	-1.2928	1.2459	-1.2902	1.2465	-1.2898
4.2000	0.1750	1.2930	-1.3330	1.2936	-1.3378	1.2916	-1.3345	1.2925	-1.3330
4.8000	0.2000	1.3290	-1.3650	1.3335	-1.3691	1.3287	-1.3670	1.3300	-1.3665
6.0000	0.2500	1.3840	-1.4130	1.3876	-1.4147	1.3846	-1.4122	1.3839	-1.4116
7.2000	0.3000	1.4150	-1.4340	1.4177	-1.4343	1.4147	-1.4320	1.4148	-1.4308
8.4000	0.3500	1.4320	-1.4370	1.4343	-1.4374	1.4331	-1.4343	1.4329	-1.4326
9.6000	0.4000	1.4390	-1.4170	1.4421	-1.4153	1.4396	-1.4127	1.4397	-1.4130
10.8000	0.4500	1.4320	-1.3750	1.4354	-1.3739	1.4341	-1.3717	1.4354	-1.3721
12.0000	0.5000	1.4170	-1.3060	1.4194	-1.3069	1.4177	-1.3036	1.4190	-1.3036
13.2000	0.5500	1.3870	-1.2000	1.3893	-1.2011	1.3892	-1.1971	1.3891	-1.1978
13.8000	0.5750	1.3690	-1.1260	1.3713	-1.1266	1.3702	-1.1224	1.3697	-1.1228
14.4000	0.6000	1.3450	-1.0330	1.3492	-1.0332	1.3487	-1.0284	1.3467	-1.0291
15.0000	0.6250	1.3200	-0.9140	1.3235	-0.9129	1.3225	-0.9084	1.3216	-0.9096
15.6000	0.6500	1.2880	-0.7620	1.2920	-0.7606	1.2912	-0.7569	1.2905	-0.7564
16.2000	0.6750	1.2500	-0.5940	1.2554	-0.5942	1.2543	-0.5896	1.2531	-0.5888
16.8000	0.7000	1.2110	-0.4390	1.2091	-0.4419	1.2169	-0.4370	1.2158	-0.4352
17.4000	0.7250	1.1640	-0.3010	1.1623	-0.3074	1.1737	-0.2994	1.1744	-0.2998
18.0000	0.7500	1.1130	-0.1750	1.1133	-0.1801	1.1232	-0.1697	1.1243	-0.1731
18.6000	0.7750	1.0580	-0.0650	1.0593	-0.0670	1.0675	-0.0608	1.0702	-0.0598
19.2000	0.8000	0.9930	0.0290	0.9948	0.0284	1.0032	0.0354	1.0066	0.0369
19.8000	0.8250	0.9190	0.1080	0.9224	0.1088	0.9285	0.1237	0.9327	0.1169
20.4000	0.8500	0.8330	0.1650	0.8387	0.1685	0.8446	0.1772	0.8472	0.1755
21.0000	0.8750	0.7380	0.2030	0.7440	0.2064	0.7494	0.2154	0.7518	0.2150
21.6000	0.9000	0.6250	0.2110	0.6317	0.2147	0.6371	0.2211	0.6412	0.2231
22.2000	0.9250	0.4980	0.1870	0.5046	0.1920	0.5076	0.2004	0.5140	0.1988
22.8000	0.9500	0.3500	0.1190	0.3574	0.1255	0.3580	0.1314	0.3632	0.1333
23.4000	0.9750	0.1790	-0.0010	0.1864	0.0053	0.1829	0.0104	0.1895	0.0128
24.0000	1.0000	-0.0190	-0.1870	-0.0077	-0.1765	-0.0217	-0.1796	-0.0184	-0.1734

Table 2. Concluded.

		Measured Values				Design Values
		y = 38.932 in		y = 45.948 in		Wing Tip Radius
x, in	x/c	z_u, in	z_l, in	z_u, in	z_l, in	R, in.
0.0000	0.0000	0.0000	0.0000	0.0000	0.0000	0.000
0.1800	0.0075	0.4580	-0.4583	0.4648	-0.4585	0.461
0.3000	0.0125	0.5625	-0.5640	0.5681	-0.5613	0.564
0.6000	0.0250	0.7248	-0.7321	0.7250	-0.7271	0.729
0.9000	0.0375	0.8299	-0.8446	0.8316	-0.8402	0.837
1.2000	0.0500	0.9103	-0.9320	0.9109	-0.9273	0.923
1.8000	0.0750	1.0330	-1.0639	1.0301	-1.0552	1.050
2.4000	0.1000	1.1199	-1.1560	1.1161	-1.1480	1.141
3.0000	0.1250	1.1900	-1.2284	1.1842	-1.2206	1.214
3.6000	0.1500	1.2454	-1.2836	1.2417	-1.2780	1.268
4.2000	0.1750	1.2929	-1.3283	1.2887	-1.3270	1.313
4.8000	0.2000	1.3324	-1.3631	1.3308	-1.3633	1.347
6.0000	0.2500	1.3833	-1.4117	1.3877	-1.4143	1.398
7.2000	0.3000	1.4138	-1.4310	1.4174	-1.4363	1.424
8.4000	0.3500	1.4310	-1.4283	1.4336	-1.4394	1.434
9.6000	0.4000	1.4369	-1.4073	1.4397	-1.4176	1.428
10.8000	0.4500	1.4329	-1.3670	1.4362	-1.3743	1.403
12.0000	0.5000	1.4168	-1.3004	1.4208	-1.3049	1.361
13.2000	0.5500	1.3876	-1.1963	1.3909	-1.1989	1.293
13.8000	0.5750	1.3689	-1.1224	1.3708	-1.1250	1.248
14.4000	0.6000	1.3461	-1.0287	1.3476	-1.0315	1.189
15.0000	0.6250	1.3204	-0.9091	1.3215	-0.9128	1.117
15.6000	0.6500	1.2891	-0.7564	1.2893	-0.7598	1.025
16.2000	0.6750	1.2520	-0.5891	1.2509	-0.5927	0.922
16.8000	0.7000	1.2128	-0.4338	1.2144	-0.4376	0.825
17.4000	0.7250	1.1698	-0.2965	1.1687	-0.3019	0.732
18.0000	0.7500	1.1225	-0.1706	1.1209	-0.1761	0.644
18.6000	0.7750	1.0688	-0.0577	1.0665	-0.0598	0.561
19.2000	0.8000	1.0052	0.0397	1.0004	0.0357	0.482
19.8000	0.8250	0.9320	0.1198	0.9280	0.1171	0.405
20.4000	0.8500	0.8493	0.1811	0.8447	0.1753	0.334
21.0000	0.8750	0.7546	0.2194	0.7506	0.2131	0.267
21.6000	0.9000	0.6446	0.2282	0.6387	0.2184	0.207
22.2000	0.9250	0.5153	0.2058	0.5083	0.1999	0.155
22.8000	0.9500	0.3661	0.1395	0.3586	0.1306	0.115
23.4000	0.9750	0.1892	0.0174	0.1809	0.0091	0.090
24.0000	1.0000	-0.0061	-0.1671	-0.0139	-0.1757	0.084

Table 3. Static Test Cases for the Rectangular Supercritical Wing

Test Case No.	Point	M	α_{o}, deg.	Comments
6E1	212	.404	2.22	
6E2	394	.604	2.00	
6E3	364	.701	2.00	
6E4	331	.753	2.05	Versus
6E5	152	.802	2.00	M @ $\alpha_o = 2°$
6E6	462	.828	2.00	
6E7	276	.850	2.01	
6E8	423	.876	2.00	
6E9	251	.907	2.00	
6E10	489	.803	1.99	Repeat of 152
6E11	214	.403	.21	
6E12	154	.801	.03	Versus
6E13	464	.821	-.01	M @ $\alpha_o = 0°$
6E14	253	.901	.00	
6E15	210	.403	4.20	
6E16	150	.803	3.99	Versus
6E17	460	.828	4.00	M @ $\alpha_o = 4°$
6E18	249	.903	4.00	
6E19	604	.400	7.01	Versus
6E20	607	.400	9.97	α_o @ M=.4
6E21	609	.401	12.00	
6E22	628	.826	.00	With transition
6E23	626	.825	2.00	strip
6E24	624	.826	4.00	
6E25	52	.802	-.05	
6E26	53	.802	2.01	Air
6E27	54	.801	4.01	

Table 4. Dynamic Test Cases for the Rectangular Supercritical Wing

Test Case No.	Point	M	q psf	α_o deg.	θ deg.	f Hz	k	Comments
6E28	514	.402	54.8	1.97	1.003	10.00	.309	Versus M @ $\alpha_o = 2^o$
6E29	344	.750	100.8	2.05	1.052	14.99	.249	
6E30	316	.802	107.6	2.08	1.035	15.03	.233	
6E31	475	.826	108.1	1.97	1.023	15.01	.228	
6E32	289	.854	113.7	1.99	1.006	14.96	.219	
6E33	435	.875	115.2	1.96	.987	14.99	.215	
6E34	264	.894	116.8	2.01	1.032	14.99	.210	
6E35	513	.403	54.7	1.97	1.008	5.02	.155	vs k, $\alpha_o = 2^o$ M = .40
6E36	515	.402	54.7	1.98	1.020	15.06	.466	
6E37	516	.402	54.8	1.98	1.060	19.97	.617	
6E38	494	.803	106.1	2.19	1.069	1.98	.031	Versus k @ $\alpha_o = 2^o$ M = .80
6E39	493	.802	105.8	1.89	1.025	3.00	.047	
6E40	495	.803	106.1	1.84	1.080	3.95	.062	
6E41	314	.803	107.7	2.10	1.080	4.95	.077	
6E42	315	.804	107.9	2.08	1.057	9.96	.154	
6E43	317	.802	107.5	2.07	1.039	20.01	.311	
6E44	473	.825	107.8	1.98	1.070	4.97	.076	Versus k @ $\alpha_o = 2^o$ M = .825
6E45	474	.825	107.8	1.97	1.038	9.96	.152	
6E46	476	.825	108.0	1.97	1.035	20.07	.305	
6E47	262	.896	117.1	2.00	1.022	4.96	.069	Versus k @ $\alpha_o = 2^o$ M = .90
6E48	263	.896	117.1	2.00	.989	9.95	.139	
6E49	265	.902	118.3	2.01	1.055	19.99	.278	
6E50	481	.823	107.6	-.03	1.023	15.01	.229	Versus α_o,@ M = .825
6E51	469	.822	107.2	3.99	1.018	15.04	.230	
6E52	269	.901	118.2	-.03	1.065	14.98	.208	Versus α_o @ M = .90
6E53	258	.900	117.9	4.03	1.024	14.95	.208	
6E54	632	.825	108.7	1.98	1.014	10.03	.152	With Transition Strip, M = .825
6E55	633	.826	108.9	1.98	.984	15.03	.228	
6E56	634	.826	108.9	1.98	1.005	20.09	.305	
6E57	180	.802	108.0	3.30	.500	15.12	.234	Versus θ @ α_o= 3.3° M = .80
6E58	184	.801	107.8	3.30	.983	15.03	.233	
6E59	189	.802	108.2	3.29	1.513	14.99	.232	
6E60	613	.402	54.4	11.99	1.004	5.00	.155	Versus k, @ α_o= 12° M = .40
6E61	614	.401	54.2	12.00	.998	10.02	.312	
6E62	615	.401	54.2	12.01	1.012	14.99	.466	
6E63	616	.401	54.3	12.02	1.087	19.99	.621	

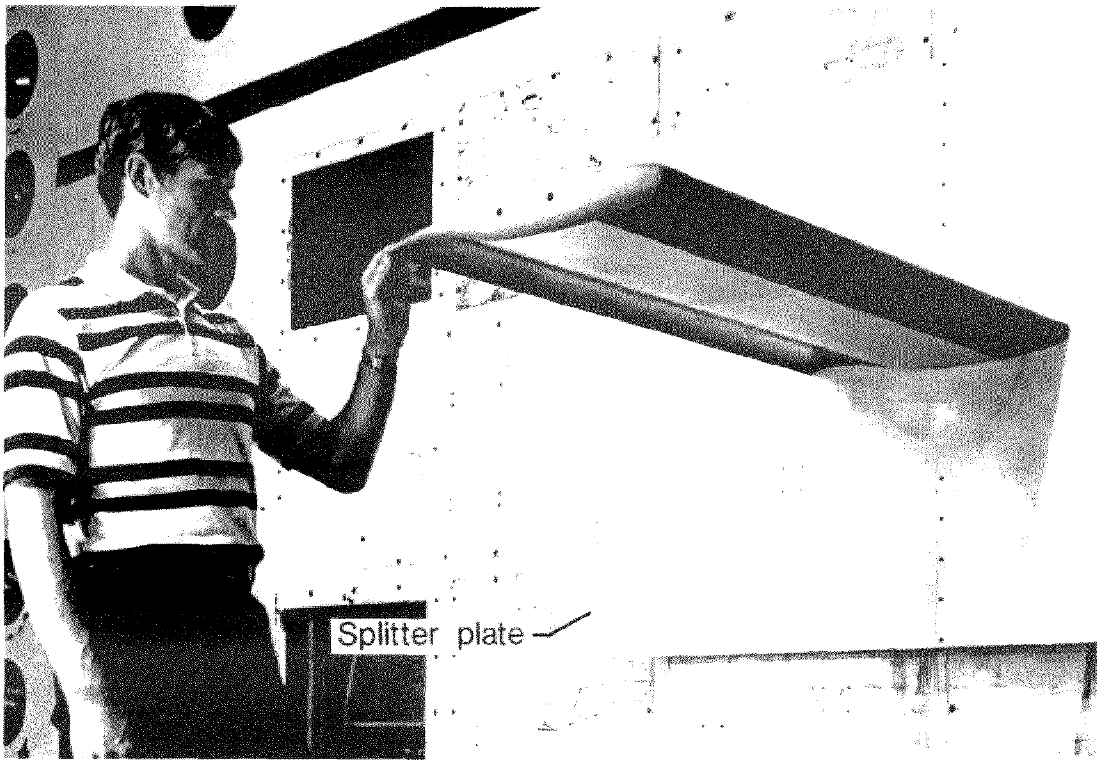

Figure 1. Rectangular supercritical wing installed in wind tunnel.

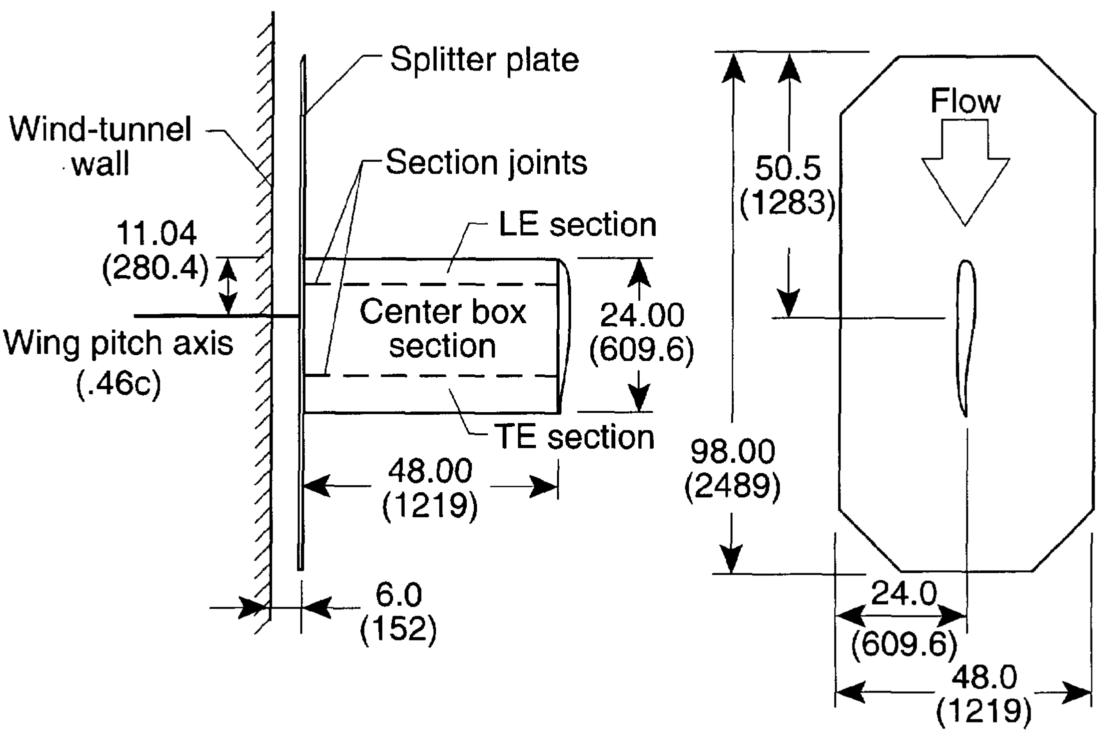

Figure 2. Diagram of wing and splitter plate in wind tunnel. Dimensions in inches (mm).

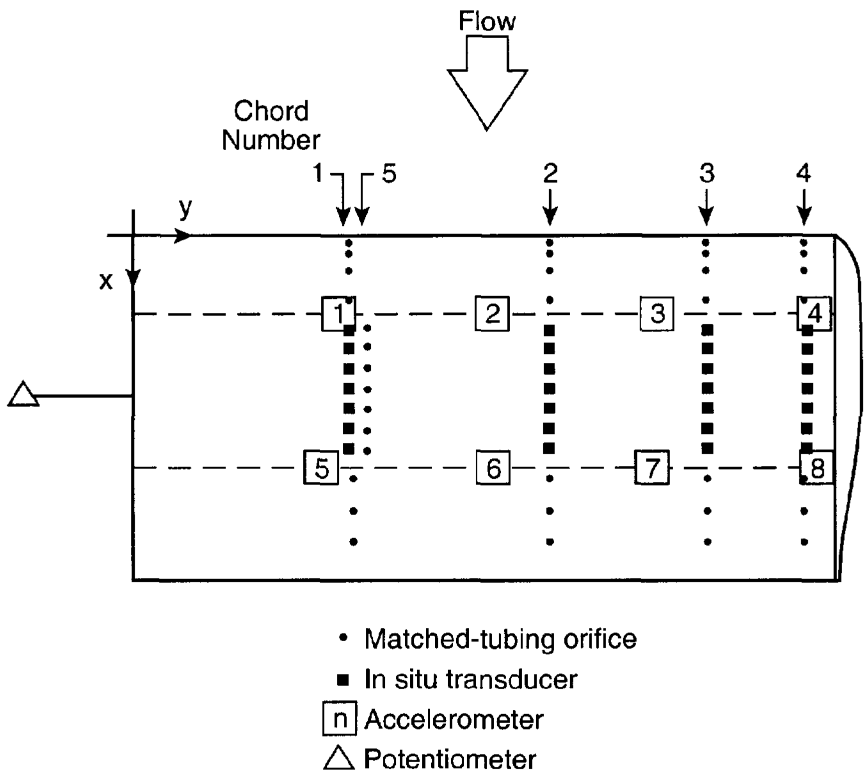

Figure 3. Instrumentation layout for the RSW model.

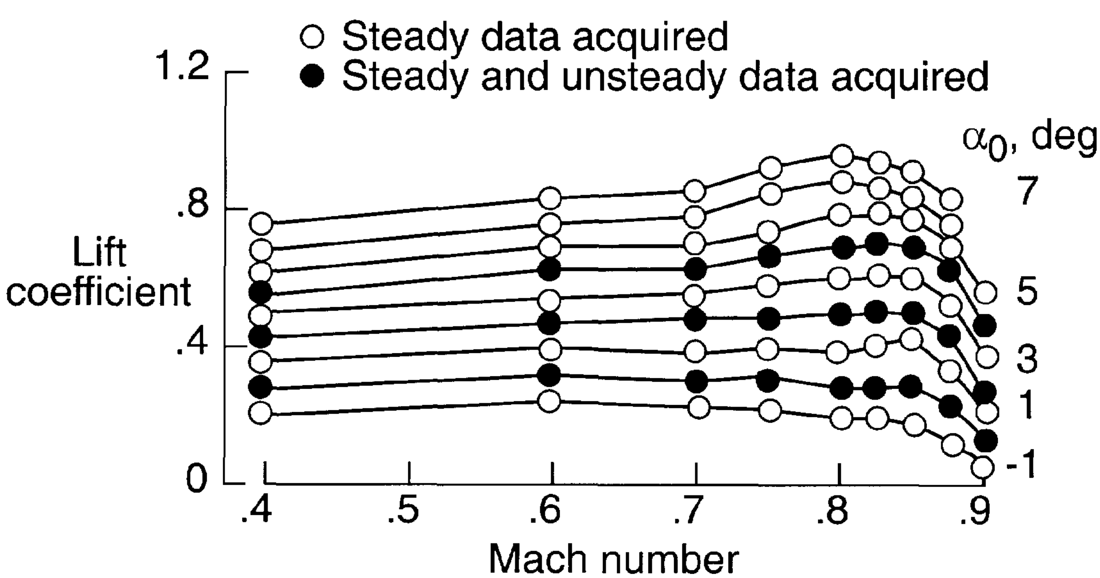

Figure 4. Lift coefficient vs. Mach number.

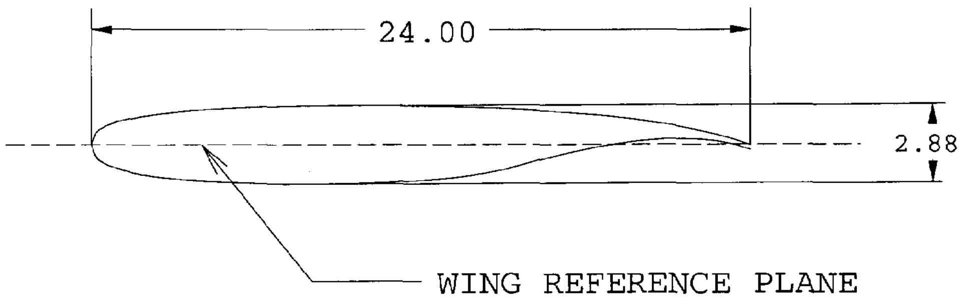

Figure 5. Airfoil for rectangular supercritical wing.

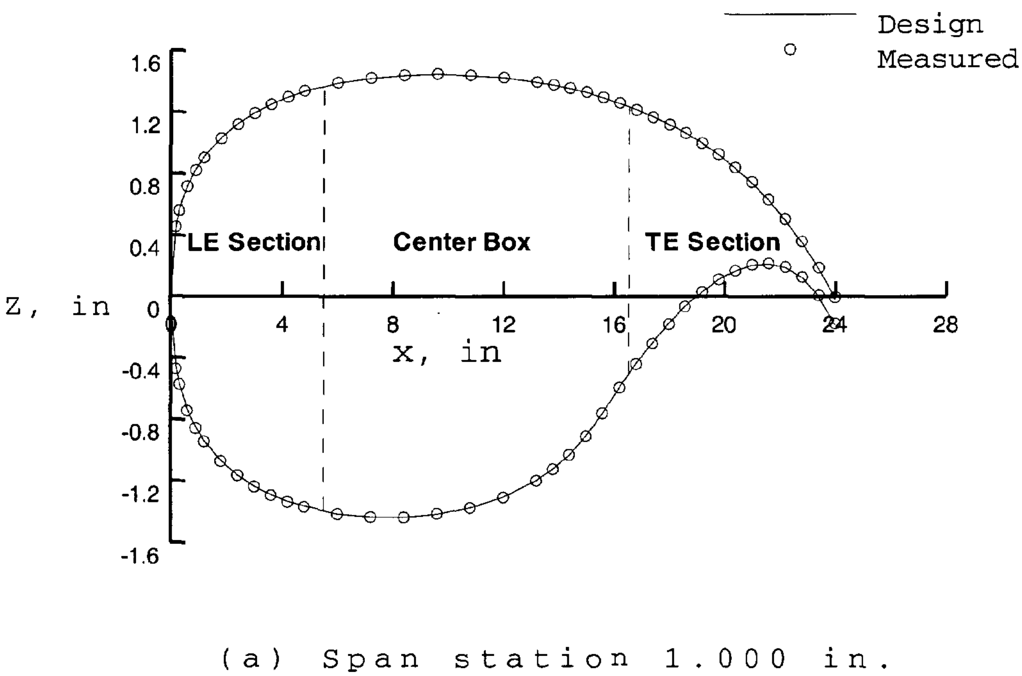

Figure 6. Comparison of the design and measured coordinates.

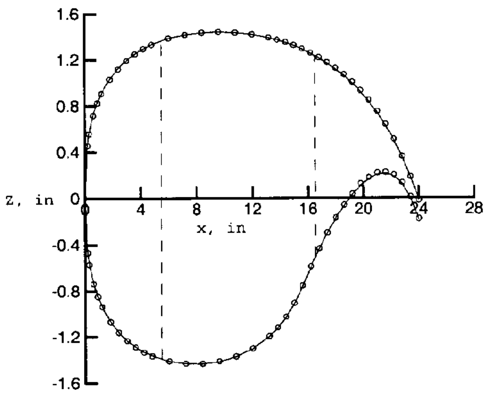

(b) Span station 14.932 in.

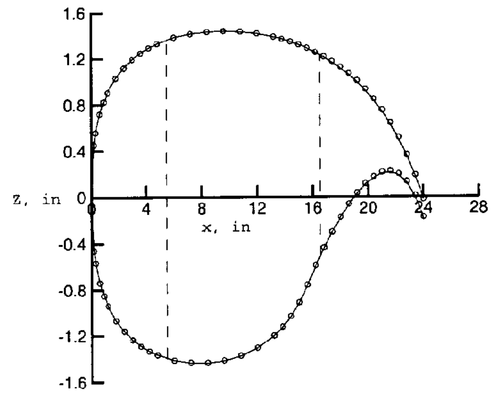

(c) Span station 28.324 in.

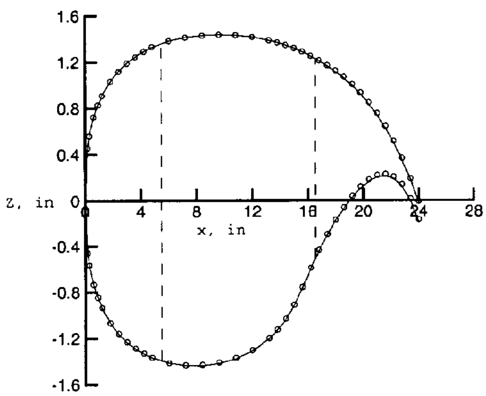

(d) Span station 38.932 in.

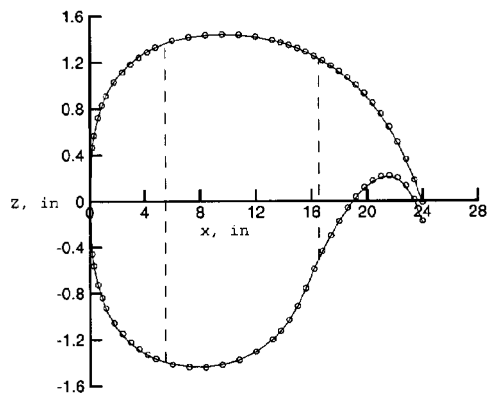

(e) Span station 45.948 in.

Figure 6. Concluded.

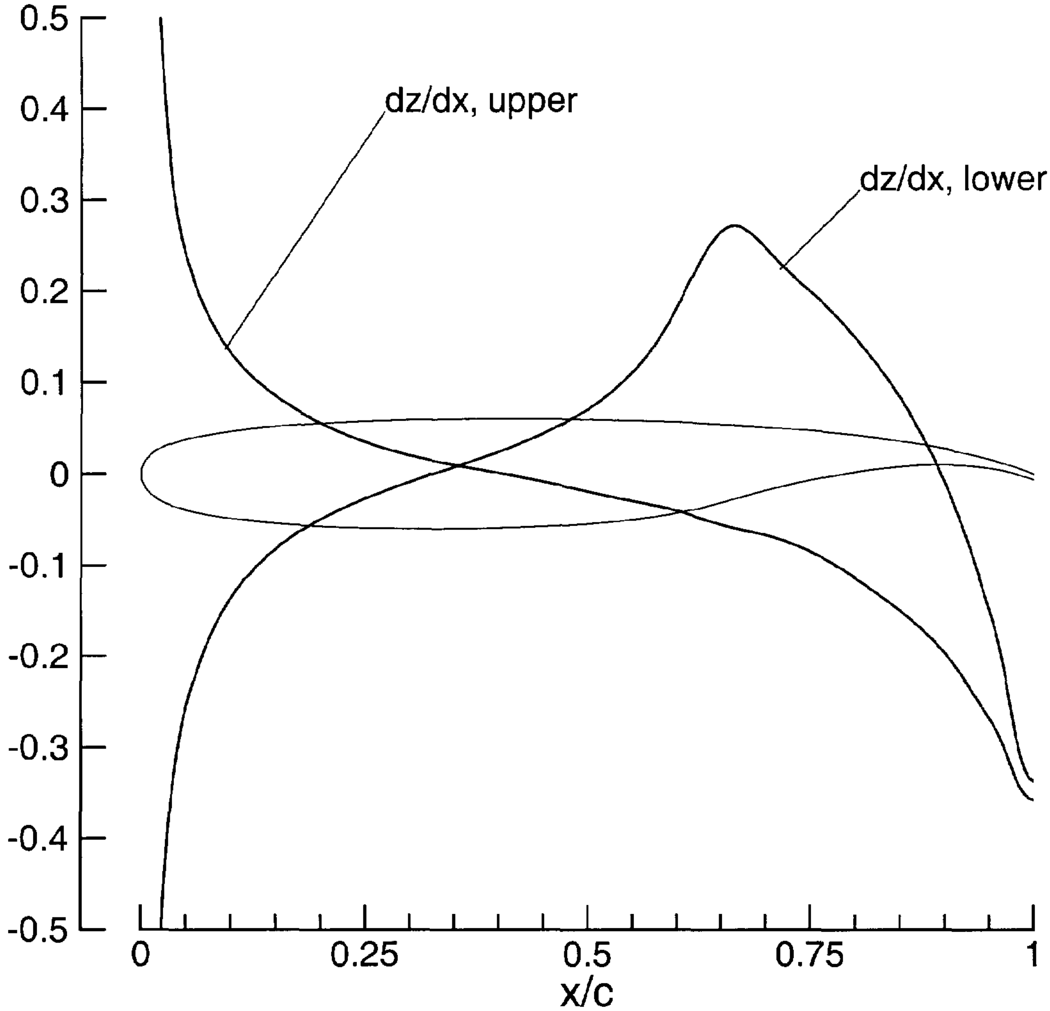

Figure 7. Plot of interpolated ordinates and slopes of smoothed measured airfoil, y = 28.324 in.

Point Number = 152 Mach Number = 0.802 Alphao = 2.00, deg.

q	H	V	Rn	gamma	Cp*
106.1	415.9	403.5	.401E+07	1.133	-0.479

	y/s =0.309		y/s =0.588		y/s =0.809		y/s =0.951	
x/c	Cpu	Cpl	Cpu	Cpl	Cpu	Cpl	Cpu	Cpl
.000	1.187		1.164		1.166		1.159	
.025	-0.666	-0.092	-0.826	-0.151	-0.845	-0.117	-0.739	-0.156
.050	-0.906	-0.310	-0.857	-0.201	-0.944	-0.307	-0.995	-0.398
.100	-0.930	-0.399	-0.904	-0.381	-0.961	-0.460	-0.824	-0.416
.200	-0.907	-0.350	-0.897	-0.414	-0.874	-0.362	-0.429	-0.370
.260	-0.936	-0.378	-0.945	-0.399	-0.362	-0.324	-0.340	-0.345
.320	-0.849	-0.296	-0.841	-0.314	-0.336	-0.283	-0.265	-0.274
.380	-0.471	-0.289	-0.230	-0.359	-0.323	-0.292	-0.263	-0.247
.440	-0.183	-0.329	-0.318	-0.269	-0.310	0.000	-0.275	-0.313
.500	-0.404	-0.344	-0.391	-0.366	-0.342	-0.366	-0.249	-0.303
.560	-0.444	-0.291	-0.374	-0.398	-0.358	-0.331	-0.230	-0.335
.620	-0.511	-0.013	-0.451	-0.093	-0.373	-0.113	-0.226	-0.193
.700	-0.550	0.260	-0.522	0.258	-0.402	0.204	-0.258	0.130
.800	-0.608	0.392	-0.553	0.440	-0.478	0.335	-0.313	0.314
.900	-0.319	0.499	-0.353	0.602	-0.338	0.478	-0.396	0.393

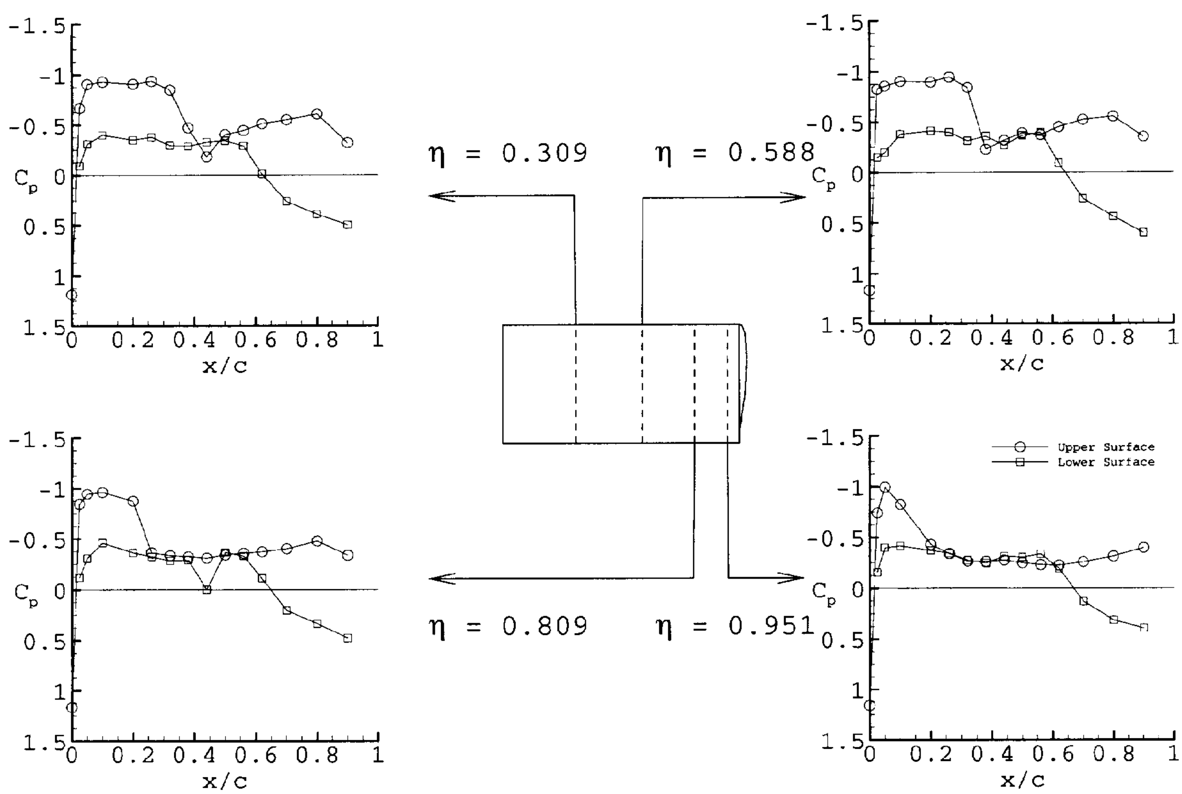

Figure 8. Sample static data, Test Case 6E3 (point 152).

Point Number = 315 Mach Number = 0.804 Alphao = 2.08, deg.

q,psf	H,psf	V,fps	Rn	gamma	freq,Hz	k	theta,deg
107.9	422.2	405.5	.401E+07	1.131	9.96	0.154	1.057

	y/s = 0.309				y/s = 0.588			
x/c	ReCpu/t	ImCpu/t	ReCpl/t	ImCpl/t	ReCpu/t	ImCpu/t	ReCpl/t	ImCpl/t
.000	-0.492	0.426			-0.569	0.415		
.025	-6.080	3.343	6.761	-2.800	-4.855	2.758	6.959	-3.026
.050	-6.356	3.626	6.721	-2.895	-7.377	4.022	6.142	-2.594
.100	-5.686	3.270	6.260	-2.131	-5.373	2.942	5.600	-2.049
.200	-5.786	3.830	4.620	-0.948	-5.532	3.524	4.146	-0.828
.260	-7.307	5.251	3.740	-0.059	-11.959	7.560	3.402	0.292
.320	-14.397	10.888	3.183	0.312	-18.215	9.849	2.634	0.342
.380	-16.559	10.428	2.602	0.534	-10.416	5.917	2.142	0.594
.440	-9.467	0.596	2.046	0.533	2.422	-6.618	1.822	0.699
.500	1.327	-8.571	1.499	0.630	1.672	-5.610	1.001	0.831
.560	2.087	-7.183	0.430	1.170	1.173	-4.231	0.249	1.055
.620	1.942	-3.998	-1.187	1.616	1.015	-3.033	-0.489	1.147
.700	2.124	-2.604	1.623	0.105	0.793	-1.294	0.972	0.340
.800	1.269	1.183	2.228	-0.851	0.773	0.595	1.582	-0.711
.900	-0.369	1.750	1.710	-1.048	-0.332	1.647	1.330	-0.838

	y/s = 0.809				y/s = 0.951			
x/c	ReCpu/t	ImCpu/t	ReCpl/t	ImCpl/t	ReCpu/t	ImCpu/t	ReCpl/t	ImCpl/t
.000	-0.550	0.348			-0.465	0.279		
.025	-4.582	2.467	5.469	-2.514	-6.241	3.031	5.484	-2.050
.050	-7.607	4.165	5.454	-2.269	-5.423	2.847	5.467	-1.936
.100	-4.777	2.562	3.519	-1.822	-7.007	3.679	3.604	-0.773
.200	-10.130	7.360	1.776	-0.372	-2.313	0.581	1.789	0.009
.260	-9.064	4.539	1.191	0.152	-2.847	0.678	1.096	0.470
.320	-1.827	-1.448	0.958	0.345	-1.662	-0.245	-0.027	0.975
.380	-1.387	-1.737	0.698	0.638	-1.358	-0.546	0.625	0.430
.440	-0.870	-1.807	-0.554	0.000	-0.988	-0.761	0.356	0.478
.500	-0.319	-2.035	0.463	0.647	-0.569	-0.792	0.063	0.647
.560	0.012	-1.735	-0.063	0.971	-0.210	-0.785	-0.219	0.612
.620	0.195	-1.505	-0.750	1.078	0.012	-0.705	-0.828	0.613
.700	0.253	-0.942	0.292	0.380	-0.033	-0.487	0.061	0.319
.800	0.050	0.649	0.538	-0.168	-0.990	0.286	0.542	0.012
.900	-0.179	0.904	0.249	-0.536	-3.406	1.545	0.257	0.085

(a) Tabulated data for Test Case 6E42

Figure 9. Sample data for pitch oscillation, Test Case 6E42 (point 315).

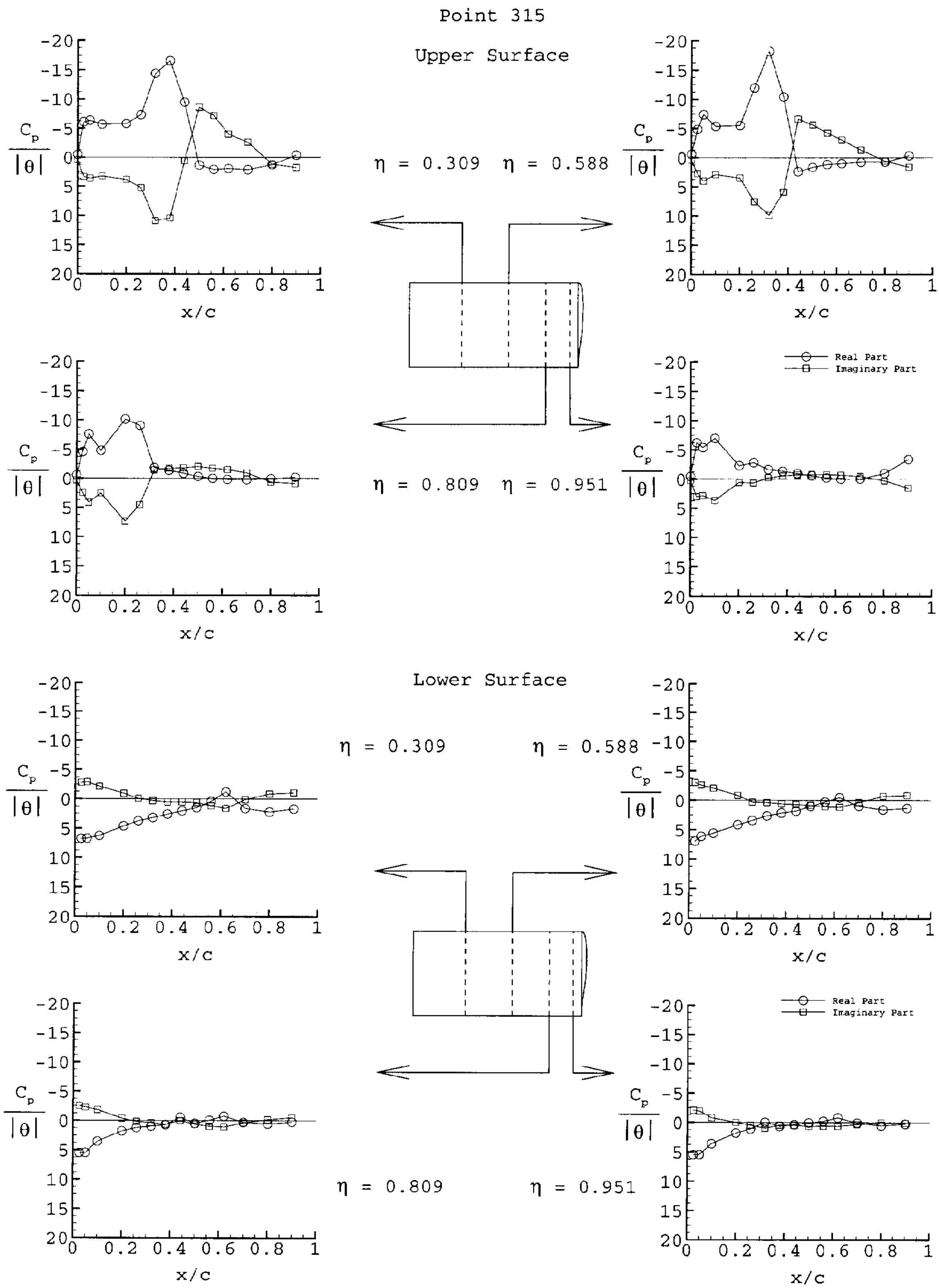

(b) Plot of data for Test Case 6E42
Figure 9. Concluded.